



Research paper

Designing a new robust control for virtual inertia control in the microgrid with regard to virtual damping

F. Amiri, M.H. Moradi*

Department of Electrical Engineering, Bu-Ali Sina University, Hamedan, Iran.

Article Info

Article History:

Received 20 March 2019
Reviewed 08 May 2019
Revised 04 September 2019
Accepted 06 December 2019

Keywords:

A new robust control method
Output feedback
Virtual inertia control
The islanded microgrid

*Corresponding Author's Email
Address:

mh_moradi@yahoo.co.uk

Abstract

Background and Objectives: Virtual inertia control, as a component of a virtual synchronous generator, is used for the implementation of synchronous generator behaviour in microgrids. In microgrids that include high-capacity distributed generation resources, in addition to virtual inertia, virtual damping can also lead to improvement of frequency stability of the microgrid. The purpose of the control method for the islanded microgrid is to be: 1) robust to the uncertainty of the microgrid parameters. 2) Weaken the disturbances on the islanded microgrid (wind turbine, solar cell, Loads). 3) Improved response speed related to microgrid frequency deviation (reduced settling time).

Methods In this paper, designing a new robust control method for controlling virtual inertia in microgrids, with regard to virtual damping, has been attempted. The proposed method has a higher degree of freedom compared to the conventional robust controllers, which provides better control of the system.

Results: Results of the proposed method for virtual inertia control with regard to virtual damping has been compared in several scenarios –with virtual inertia control based on optimized PI controllers with regard to virtual damping, virtual inertia control based on model predictive control (controller) with regard to virtual damping, Self-adaptive virtual inertia control using fuzzy logic, virtual inertia control with regard to virtual damping, and virtual inertia control without virtual damping (conventional methods). Compared to other control methods, the proposed controller has improved the settling time due to the frequency deviations of the islanded microgrid by 27%. According to the results of the scenarios, the proposed controller has been able to reduce the frequency error due to load and distributed generation resource disturbances and compared to other controllers, and this frequency deviation has been reduced by 68%.

Conclusion: According to the simulation results, the proposed controller has a better performance than other controllers in improving the frequency stability of the islanded microgrid.

©2020 JECEI. All rights reserved.

Introduction

Due to the increasing need for power generation, the distributed generation resources have penetration into the power system and have gradually replaced

conventional systems [1], [2]. Wind Turbines and solar cells (Photovoltaic) are among the most widely used sources of production in the power system [3], [4]. Since these sources exchange power with the microgrid

through power electronic converters, when a disturbance occurs in the microgrid, it causes higher frequency and voltage deviations in the system due to the low inertia of the system (power electronic converters) [5], [6]. Increasing the capacity of distributed generation sources such as wind turbines and Photovoltaic (PV) in the microgrids more and more will cause many problems in the stability of voltage and frequency due to the lack of inertia, compromising the stability of the microgrid [7]-[9]. Thus, the concept of the virtual synchronous generator (VSG) in the microgrid was introduced to implement the behavior of synchronous generators of the power system. Implementing this method improves the inertia, output impedance, and stability of the microgrid [10]-[12].

Virtual inertia control is a special part of the virtual synchronous generator (VSG). The virtual inertia control can be implemented on energy storage systems (ESS), enabling them to operate like traditional synchronous generators. As a primary stimulus, the virtual inertia control can improve the frequency stability with the occurrence of disturbances in the microgrid [13], [14]. In microgrids, in addition to virtual inertia, the existence of virtual damping can help improve frequency stability. For example, when load disturbance occurs, virtual inertia, as a prime mover, prevents too much frequency decline, and the existence of virtual damping provides more damping to the microgrid (Fast damping of fluctuations). Various control methods have been used for virtual inertia to improve the frequency stability of the islanded microgrid. The control method used for virtual inertia must meet the following objectives.

- 1) It is robust to the uncertainty of the microgrid parameters.
- 2) Weaken the effect of disturbance on the microgrid frequency.
- 3) Improve the response speed to the islanded microgrid frequency deviations.

Control methods for virtual inertia control in the islanded microgrid can be divided into two categories: 1) Controller design for virtual inertia control without considering virtual damping [15]-[24]. 2) Controller design for virtual inertia with considering virtual damping [25].

In [15], the PI controller (proportional-integral controller) has been used to control virtual inertia control in the AC/DC microgrid. A control method for an electric vehicle has been provided in the microgrid based on the virtual inertia control method using a PI controller [16]. The PI controller used for virtual inertia does not perform well against the uncertainty of microgrid parameters as well as disturbances. In [17], the researchers have employed the coefficient diagram method as a robust controller to virtual inertia control in

the islanded microgrids. The coefficient diagram method used for virtual inertia performs well against the uncertainty of microgrid parameters but does not perform well in attenuation of disturbance. In [18], an adaptive control method has been applied to virtual inertia control in the microgrid to improve frequency stability. The adaptive control method is robust to disturbance and uncertainty of microgrid parameters, but the response speed does not well. In [19], the researchers have focused on the design of a neural-fuzzy controller to virtual inertia control in the islanded microgrids. The neural-fuzzy controller is unable to weaken the disturbances on the islanded microgrid. In [20], an H^∞ controller has been designed to virtual inertia control in the microgrid with the influence of distributed generation sources. In [21], it has been focused on the design of Adaptive Virtual Inertia Control-Based Fuzzy Logic in the microgrid with the influence of distributed generation sources aimed at improving frequency stability. In [22], the researchers have designed an H^∞ controller to the virtual inertia control in the microgrid by considering the phase-locked loop in the microgrid model. The control methods used in [22] are robust to disturbance and uncertainty of microgrid parameters, but the settling time (response speed) of the islanded microgrid frequency deviations is long. In [23], a model predictive control (controller) has been designed to the virtual inertia control in the microgrid targeted to improve frequency stability. The model predictive control (controller) performs well against disturbances, but is not relatively robust to the uncertainty of microgrid parameters. A virtual inertia controller has been designed for an islanded microgrid with two areas in [24]. In [25], virtual inertia control with regard to virtual damping has been designed for islanded microgrids. The control method used in [25] has a good settling time (response speed) but is not robust to disturbances and uncertainty of island microgrid parameters. Therefore, it is necessary to have a proper control method that can be resistant to the uncertainty of the parameters of the islanded microgrid and can weaken high disturbances and also have a suitable response speed. In this paper, a new robust control method of output feedback based on linear matrix inequality for virtual inertia control with regard to virtual damping for the islanded microgrids has been utilized. The proposed control method does not require measuring of all the modes and uses only output feedback. The proposed method has a higher degree of freedom compared to the conventional robust controllers, which provides better control of the system. In the proposed method, all the uncertainties related to the microgrid parameters are considered and the criterion for weakening the disturbance is also

considered in it. The purpose of the control method is to be: 1) robust to the uncertainty of the microgrid parameters. 2) Weaken the disturbances on the islanded microgrid (wind turbine, solar cell, Loads). 3) Improved response speed related to microgrid frequency deviation (reduced settling time). Results of the proposed method for virtual inertia control with regard to virtual damping has been compared in several scenarios - with the consideration of the uncertainty of islanded microgrid parameters as well as disturbances imposed upon the microgrid - to virtual inertia control based on optimized PI controllers with regard to virtual damping, virtual inertia control based on model predictive control (controllers) with regard to virtual damping, Self-adaptive virtual inertia control using fuzzy logic, virtual inertia control with regard to virtual damping, and virtual inertia control without virtual damping (conventional methods), and performance of the proposed method with respect to response speed, decrease in frequency deviation, and robustness to parameter uncertainty and disturbances imposed upon the islanded microgrid is shown. The proposed method has been verified based on Lyapunov's criteria. Simulation has been performed in Matlab Software.

The article includes the islanded microgrid structure, designing a new robust controller for islanded microgrids, simulation, and conclusion.

Microgrid Structure

A. Virtual inertia control with regard to virtual damping on the islanded microgrid

The objective of designing a virtual inertia control system is providing the appropriate virtual inertia and damping in microgrids that possess vast distributed generation resources. Since this microgrid does not possess adequate inertia in comparison to power systems, this control section operates as a separate control section to maintain microgrid frequency stability in the transient and steady states [15]-[24]. In Fig. 1, the dynamic model (microgrid) of virtual inertia control with consideration of virtual damping is shown. The virtual inertia control is a derivative control in which the frequency variations rate is added as the additional active power to the reference microgrid during disturbances and incidents acting on the microgrid. Virtual damping has also been used for more rapid damping of microgrid frequency deviation [17], [25]. The derivative control, which is highly sensitive to the frequency measurement noises, uses a low-pass filter to solve this problem. The low-pass filter simulates the behavior of an energy storage system (ESS) [17].

Therefore, virtual inertia control with regard to virtual damping prevents microgrid frequency instability and improves microgrid inertia and damping.

B. Components of the islanded microgrid

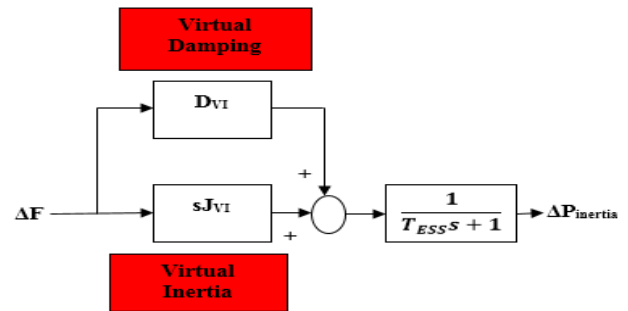


Fig. 1: Dynamic model of virtual inertia control in the microgrid with regard to virtual damping [25].

Fig. 2 shows the structure of the islanded microgrid. The studied microgrid consists of a 15 MW of a thermal power plant, 7.5 MW of a solar farm, 8.5 MW of a wind farm, and 4.5 MW of energy storage system (ESS). The microgrid also consists of two types of load: 10 MW of industrial load and 5 MW of a residential load [25]. Virtual inertia control with consideration of virtual damping is implemented to the energy storage system, as a compensator, is expected to support the load-frequency control system in keeping a balance between production and consumption in the microgrid [20]. The dynamic model of the islanded microgrid is shown in Fig. 3. The model used for the islanded microgrid components was a reduced-order model, which is a proper model for frequency stability analysis in microgrids. According to Fig. 3, three control structures were considered to enable the islanded microgrid function well against disturbances and improve the frequency stability in the islanded microgrid: virtual inertia control, Primary control and secondary control (LFC) [18]-[25]. For designing a controller for virtual inertia control with consideration of virtual damping in the islanded microgrid, at first, the state-space model of the islanded microgrid was attained, and was proceeded with designing the proposed control method for virtual inertia control with consideration of the microgrid virtual damping.

C. State-space model of the islanded microgrid

The state-space model of the islanded microgrid for virtual inertia control with regard to virtual damping to improve the frequency stability is shown as (1). The disturbances on the islanded microgrid are shown in (2) [22]-[25]. In (1) and (2), Δf is the microgrid frequency deviation. ΔP_w is the generated from the wind turbine. ΔP_g is generated from the governor. ΔP_{ACE} is generated from the area control. $\Delta P_{inertia}$ is generated from virtual inertia power. ΔP_{pv} is generated from the solar power. ΔP_l is commercial load power, and ΔP_R is residential load power.

Designing a new robust controller for virtual inertia control with consideration of virtual damping

A. The proposed controller structure

The new robust control method has been designed for virtual inertia control with consideration of virtual damping in the islanded microgrid. The controller structure is designed in such a way that there is the uncertainty of parameters and disturbance in the studied islanded microgrid. Also, we cannot measure all states and modes, and even if it can, it will cost more due to the need for more sensors. The control system is designed in such a way that the islanded microgrid

would be free of external disturbances and under the uncertainty of parameters with an asymptote stable output feedback and can meet the $\frac{\|z\|_{L_2}}{\|w\|_{L_2}} \leq \gamma$ criterion in

the presence of disturbances in the microgrid. The structure of the islanded microgrid (with parameter uncertainty and under disturbance) for virtual inertia control (with virtual damping) with the proposed dynamic controller is shown in Fig. 4. In Fig. 4, γ is the frequency deviation of the islanded microgrid, D is disturbance entering the islanded microgrid, and u is control signal. The dynamics of the islanded microgrid is modeled by considering the regulated output (Z) as (3).

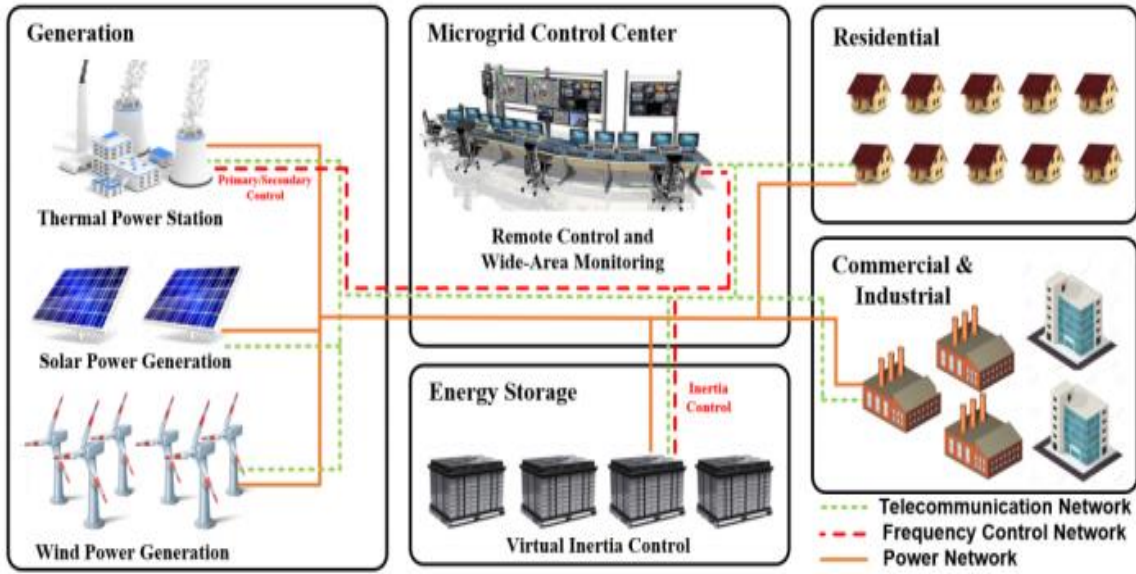


Fig. 2: The structure of the islanded microgrid [24], [25].

$$\begin{bmatrix} \Delta \dot{f} \\ \Delta \dot{P}_m \\ \Delta \dot{P}_g \\ \Delta \dot{P}_{ACE} \\ \Delta \dot{P}_{inertia} \\ \Delta \dot{P}_w \\ \Delta \dot{P}_{PV} \end{bmatrix} = \begin{bmatrix} -\frac{D}{2H} & \frac{1}{2H} & 0 & 0 & \frac{1}{2H} & \frac{1}{2H} & \frac{1}{2H} \\ 0 & -\frac{1}{T_c} & \frac{1}{T_c} & 0 & 0 & 0 & 0 \\ -\frac{1}{RT_g} & 0 & -\frac{1}{T_g} & -\frac{1}{T_g} & 0 & 0 & 0 \\ \beta K_i & 0 & 0 & 0 & 0 & 0 & 0 \\ \frac{D_{VI}}{T_{ESS}} & 0 & 0 & 0 & -\frac{1}{T_{ESS}} & 0 & 0 \\ 0 & 0 & 0 & 0 & 0 & \frac{1}{T_{WT}} & 0 \\ 0 & 0 & 0 & 0 & 0 & 0 & -\frac{1}{T_{PV}} \end{bmatrix} \begin{bmatrix} \Delta f \\ \Delta P_m \\ \Delta P_g \\ \Delta P_{ACE} \\ \Delta P_{inertia} \\ \Delta P_w \\ \Delta P_{PV} \end{bmatrix} + \begin{bmatrix} 0 \\ 0 \\ 0 \\ 0 \\ \frac{J_{VI}}{T_{ESS}} \\ 0 \\ 0 \end{bmatrix} [u] + \begin{bmatrix} 0 & 0 & -\frac{1}{2H} & -\frac{1}{2H} \\ 0 & 0 & 0 & 0 \\ 0 & 0 & 0 & 0 \\ 0 & 0 & 0 & 0 \\ 0 & 0 & 0 & 0 \\ \frac{1}{T_{WT}} & 0 & 0 & 0 \\ 0 & \frac{1}{T_{PV}} & 0 & 0 \end{bmatrix} \begin{bmatrix} \Delta P_{solar} \\ \Delta P_{wind} \\ \Delta P_i \\ \Delta P_R \end{bmatrix}$$

$$y = [1 \quad 0 \quad 0 \quad 0 \quad 0 \quad 0 \quad 0] \begin{bmatrix} \Delta f \\ \Delta P_m \\ \Delta P_g \\ \Delta P_{ACE} \\ \Delta P_{inertia} \\ \Delta P_w \\ \Delta P_{PV} \end{bmatrix} \tag{1}$$

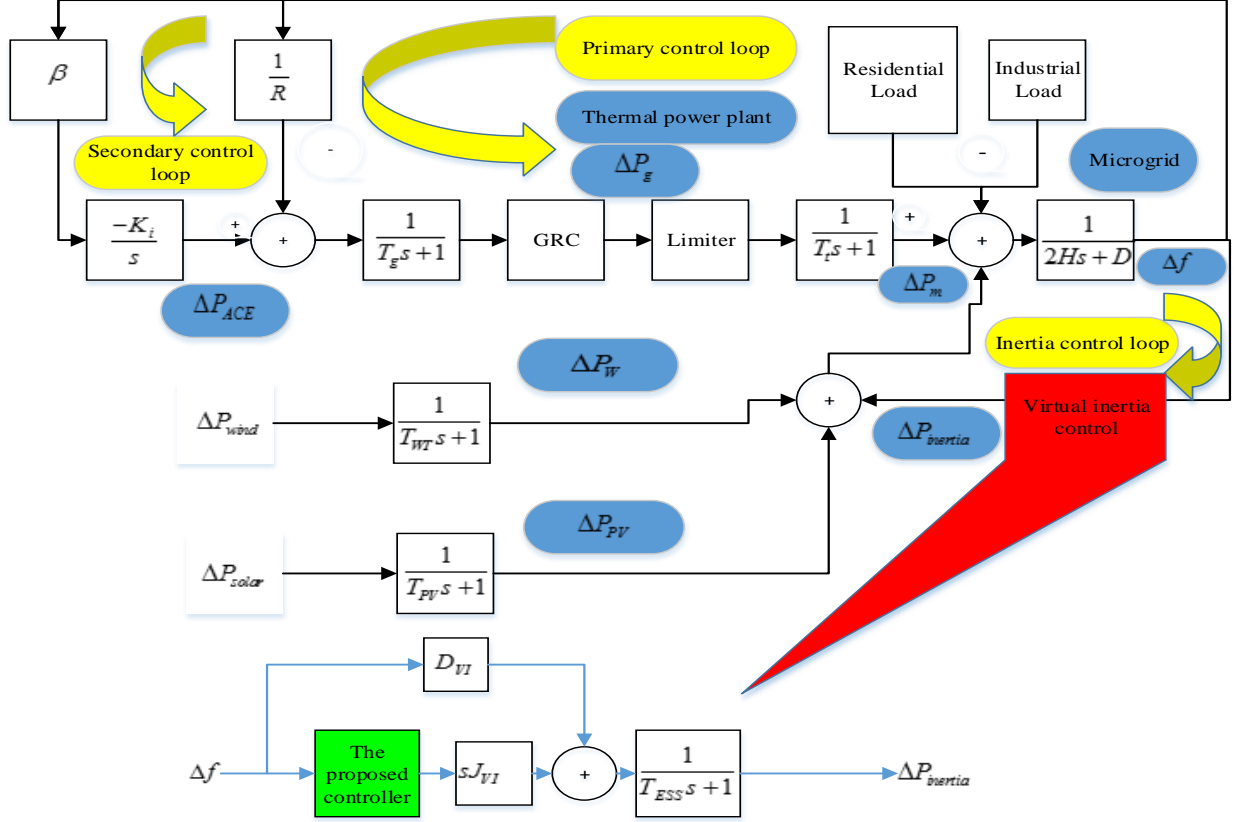


Fig. 3: The dynamic model of the islanded microgrid [23].

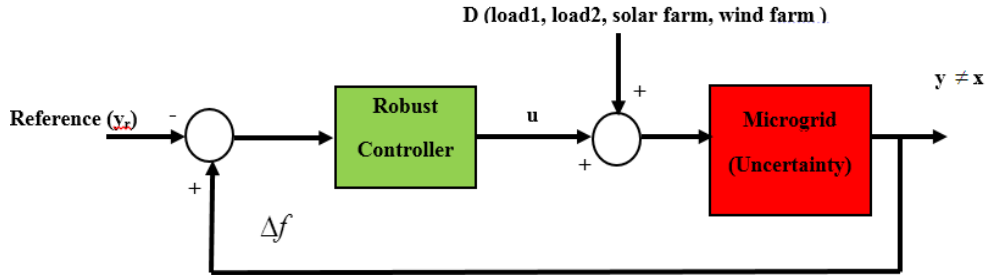


Fig. 4: The islanded microgrid structure with proposed controller.

$$w^T = [\Delta P_{solar} \quad \Delta P_{wind} \quad \Delta P_l \quad \Delta P_R] \quad (2)$$

$$\begin{aligned} \dot{x} &= A_{n \times n}(t)x_{n \times 1} + B_{n \times m}(t)u_{m \times 1} + D_{n \times d}(t)w_{d \times 1} \\ z &= C_{1_{q \times n}}(t)x_{n \times 1} + D_{11}(t)w + D_{12_{q \times m}}(t)u_{m \times 1} \\ y &= C_2(t)x_{n \times 1} + D_{21}(t)w + D_{22}(t)u \end{aligned} \quad (3)$$

Z is a virtual output that is only used for design and is selected so that it achieves the desired goals for the islanded microgrid. Z is a more general case than y (system output). In this article, z is the same as the frequency deviation of the islanded microgrid, on which the effect of disturbances (wind farm, solar farm, and load) is weakened.

In (3), $A_{n \times n}$ is the system matrix, $B_{n \times m}$ is the input matrix, $D_{n \times d}$ is the disturbance matrix, $C_{1_{q \times n}} = C_2$ is the

output matrix, n is the number of state variables, m indicates the control inputs, d is the number of disturbances, and $D_{21}(t) = D_{22}(t) = 0$. y is the linear system measurement output (frequency deviation of the islanded microgrid), and q is the number of regulated outputs [26]. Since in the islanded microgrid, $C_2 \neq I$, the robust output feedback control has been used. The variable z can be selected with regard to the control design criterion. In the proposed method, all the parameters of the linear system can be assumed uncertain, so it has been modeled as (4) [26]-[28]. The uncertainty given in (4) has been re-considered as in (5) (structure bonded), wherein $F(t)$ has been taken as 1×1 . In (5), the choice of M and N parameters is the responsibility of the designer. The structure of the dynamic controller proposed for virtual inertia control

(with consideration of virtual damping) in the islanded microgrid has uncertainty and disturbance, which is represented as (6).

$$\left. \begin{cases} A(t) = A + \Delta A(t) = A + \Delta A \\ B(t) = B + \Delta B(t) = B + \Delta B \\ D(t) = D + \Delta D(t) = D + \Delta D \\ C_1(t) = C_1 + \Delta C_1(t) = C_1 + \Delta C_1 \\ D_{12}(t) = D_{12} + \Delta D_{12}(t) = D_{12} + \Delta D_{12} \\ C_2(t) = C_2 + \Delta C_2(t) = C_2 + \Delta C_2 \end{cases} \right\} \quad (4)$$

$$\left. \begin{cases} \Delta A_{n \times n} = M_{A_{n \times n}} F_{1 \times 1}(t) N_{A_{1 \times n}} \\ \Delta D_{n \times d} = M_{D_{n \times d}} F_{1 \times 1}(t) N_{D_{1 \times d}} \\ \Delta B_{n \times m} = M_{B_{n \times m}} F_{1 \times 1}(t) N_{B_{1 \times m}} \\ \Delta C_{1_{q \times n}} = M_{C_{1_{q \times n}}} F_{1 \times 1}(t) N_{C_{1_{1 \times n}}} \\ \Delta C_{2_{p \times n}} = M_{C_{2_{p \times n}}} F_{1 \times 1}(t) N_{C_{2_{1 \times n}}} \\ \Delta D_{12_{q \times m}} = M_{D_{12_{q \times m}}} F_{1 \times 1}(t) N_{D_{12_{1 \times m}}} \\ F_{1 \times 1}^T(t) \times F_{1 \times 1}(t) \leq I, F^2(t) \leq 1 \end{cases} \right\} \quad (5)$$

$$\left. \begin{cases} \dot{\hat{x}}_{n \times 1} = \hat{A}_{n \times n} \hat{x}_{n \times 1} + \hat{B}_{n \times p} y_{p \times 1} \\ u_{m \times 1} = \hat{C}_{m \times n} \hat{x}_{n \times 1} \end{cases} \right\} \quad (6)$$

By combining (3) and (6), the closed-loop system structure (the islanded microgrid and controller) can be represented as in (7).

$$\left. \begin{cases} \dot{\hat{x}} = A(t)x + B(t)\hat{C}\hat{x} + D(t)w \\ z = C_1(t)x + D_{12}(t)\hat{C}\hat{x} \\ \dot{\hat{x}} = \hat{A}\hat{x} + \hat{B}C_2x \end{cases} \right\} \quad (7)$$

In (7), if \hat{x} and x incline toward zero, then the entire closed-loop system will be stable. Considering

$$\hat{x} = \begin{bmatrix} x \\ \hat{x} \end{bmatrix}_{2n \times 1}, \text{ Equation (7) is rewritten as (8).}$$

$$\dot{\hat{x}} = \begin{bmatrix} A(t) & B(t)\hat{C} \\ \hat{B}(t)C_2(t) & \hat{A} \end{bmatrix}_{2n \times 2n} \hat{x} + \begin{bmatrix} D(t) \\ 0 \end{bmatrix}_{2n \times d} w_{d \times 1} = \bar{A}\hat{x} + \bar{D}w \quad (8)$$

B. Objectives of the control system

For the closed-loop system (The islanded microgrid system with disturbance and parameter uncertainty and the proposed controller), there are 2 main objectives:

1. Being asymptotically stable without disturbance of the closed-loop system and under parameter

uncertainty.

2. Achieving the performance of in the presence of disturbance and uncertainty of the closed-loop system with the primary zero conditions.

In the paper, the Lyapunov stability criterion has been used to prove the stability of the proposed method. For this purpose, the Lyapunov stability criterion was applied to the islanded microgrid system with disturbance. The Lyapunov criterion and the closed-loop system structure are defined as (9). The two conditions (9(a)) and (9(c)) are essential for the stability based on the Lyapunov criterion.

$$\left. \begin{cases} v = x^T p x > 0 \Rightarrow p > 0 & (9(a)) \\ \dot{x} = Ax + Dw & (9(b)) \\ v = x^T p x + \dot{x}^T p x = x^T A^T p x + x^T p Ax + x^T p Dw < 0 & (9(c)) \end{cases} \right\} \quad (9)$$

To prove the (9(a)), meaning that $v > 0$, the matrix P, P^{-1} is defined as (10) [26]. In (10), the matrices R, T, S, and U are symmetrical because P and P^{-1} are symmetric. Meanwhile, PP^{-1} must become an identity matrix in accordance with (11).

The linearization matrix has been considered as (12) [26]. According to (12), $p\beta_1 = \beta_2$. Also, from (13) [26], the linear matrix inequality has been obtained for the first Lyapunov criterion (9(a)), meaning that if the linear matrix inequality (13) is bigger than zero, then the first criterion is met ($v > 0$).

$$p = \begin{bmatrix} S_{n \times n} & N_{n \times n} \\ N_{n \times n}^T & U_{n \times n} \end{bmatrix}, p^{-1} = \begin{bmatrix} R_{n \times n} & M_{n \times n} \\ M_{n \times n}^T & T_{n \times n} \end{bmatrix} \quad (10)$$

$$pp^{-1} = \begin{bmatrix} SR + NM^T & SM + NT \\ N^T R + UM^T & N^T M + UT \end{bmatrix} = \begin{bmatrix} I_{n \times n} & 0 \\ 0 & I_{n \times n} \end{bmatrix} \quad (11)$$

$$\beta_1 = \begin{bmatrix} R & I \\ M^T & 0 \end{bmatrix}, \beta_2 = \begin{bmatrix} I & S \\ 0 & N^T \end{bmatrix} \quad (12)$$

$$\begin{aligned} \beta_1^T p \beta_1 &= \beta_1^T \beta_2 = \begin{bmatrix} R & M \\ I & 0 \end{bmatrix} \begin{bmatrix} I & S \\ 0 & N^T \end{bmatrix} \\ &= \begin{bmatrix} R & RS + MN^T \\ I & S \end{bmatrix} = \begin{bmatrix} R & I \\ I & S \end{bmatrix} > 0 \end{aligned} \quad (13)$$

To calculate the second Lyapunov criterion (9(c)) and to convert it into a linear matrix inequality, Equations (14) to (29) have been proved.

The equation $\frac{\|z\|_{L_2}}{\|w\|_{L_2}} \leq \gamma$, which is the criterion for reduction of disturbances compared to the islanded microgrid system's states under uncertainty, has been written in accordance with (14). The objective function has been represented as the function j , and the negativity of the function j meets the second Lyapunov criterion, i.e. $\dot{v} < 0$. The upper bound for the objective function j has been obtained according to (15). If (16) exists, then the function j will be negative, and the second Lyapunov criterion will be met. Therefore, Equation (16) must be converted into a linear matrix inequality. Equation (16) has been converted, through substitution and *Schur complement*, into (17). Since P is symmetric, so $P^T = P$ and $p = \beta_2 \beta_1^{-1}$ and, accordingly, equation (17) has converted into (18). Equation (18) is not of the linear matrix inequality that can be solved by Yalmip, so it is necessary to make changes to the (18) that can be considered a linear matrix inequality. Equations (19) and (20) have been defined in order for linearizing (18). The linearization of (18) has been demonstrated in accordance with (21). By substituting (8) and (12) in (21), (22) has been obtained.

$$\begin{cases} \int_0^{\infty} z^T z dt \leq \gamma^2 \int_0^{\infty} w^T w dt \\ j = \int_0^{\infty} (z^T z - \gamma^2 w^T w) dt \leq 0 \end{cases} \quad (14)$$

$$\begin{cases} j \leq \int_0^{\infty} (z^T z - \gamma^2 w^T w) dt + v(x(\infty)) - v(x(0)) \\ j \leq \int_0^{\infty} (z^T z - \gamma^2 w^T w + \dot{v}) dt < 0 \end{cases} \quad (15)$$

$$z^T z - \gamma^2 w^T w + \dot{v} < 0 \quad (16)$$

$$\delta_1 = \begin{bmatrix} \begin{matrix} \bar{A}^T & p + p\bar{A} & p\bar{D} \\ \bar{D}p & \gamma^2 I & 0 \end{matrix} & \begin{bmatrix} C_1^T(t) \\ \hat{C}^T \\ D_{12}^T(t) \end{bmatrix} \\ \begin{bmatrix} C_1(t) & D_{12}(t)\hat{C} \end{bmatrix} & \begin{matrix} 0 & -I \end{matrix} \end{bmatrix} < 0 \quad (17)$$

$$\delta_2 = \begin{bmatrix} \begin{matrix} \bar{A}^T & \beta_2 \beta_1^{-1} + p\bar{A} & \beta_1^{-T} \beta_2^{-T} \bar{D} \\ \bar{D}\beta_2 \beta_1^{-1} & \gamma^2 I & 0 \end{matrix} & \begin{bmatrix} C_1^T(t) \\ \hat{C}^T \\ D_{12}^T(t) \end{bmatrix} \\ \begin{bmatrix} C_1(t) & D_{12}(t)\hat{C} \end{bmatrix} & \begin{matrix} 0 & -I \end{matrix} \end{bmatrix} < 0 \quad (18)$$

Subsequently, (22), after substituting (23), HAS BEEN CONVERTED INTO (24). The definitions of the parameters

$\hat{A}, \hat{B}, \hat{C}$ in (23) have been adopted from [26]-[28] and in (24), the constant parameters have been separated from the uncertain parameters by different matrices. In (24), the o matrix is linear matrix inequality, and the matrices o_1 to o_{13} are not linear matrix inequality. In (24), the matrices o_1 to o_{13} are uncertain. In order to make o_1 to o_{13} matrices appear linear matrix inequality, changes must be made in the matrices. According to (25), the above band is first defined for o_1 to o_{13} matrices. In (26), \bar{o}_1 to \bar{o}_{13} are the up band of o_1 to o_{13} matrices. Then, according to (26) and (27), the matrices \bar{o}_1 to \bar{o}_{13} are converted to linear matrix inequality. According to (27), if $\delta_4 < 0$, then $\delta_3 < 0$ and the second Lyapunov criterion will be met. In (28), for the first time, the Schur complement is used for \bar{o}_1 and entered into the o-matrix. In order for all \bar{o}_2 to \bar{o}_{13} matrices to enter the o matrix, the Schur complement is used 12 more times. And finally, the (29) is shown. Finally, Liapanov's second criterion (9-c) is shown as (29). Equation (29) is an inequality of the linear matrix in which all the uncertainties of system parameters and disturbances are modeled.

$$\begin{cases} \delta_2 < 0, \zeta^T \delta_2 \zeta < 0 \\ \zeta > 0 \end{cases} \quad (19)$$

$$\zeta = \begin{bmatrix} \beta_1 & 0 & 0 \\ 0 & I & 0 \\ 0 & 0 & I \end{bmatrix}, \zeta^T = \begin{bmatrix} \beta_1^T & 0 & 0 \\ 0 & I & 0 \\ 0 & 0 & I \end{bmatrix} \quad (20)$$

$$\delta_3 = \begin{bmatrix} \beta_1^T & 0 & 0 \\ 0 & I & 0 \\ 0 & 0 & I \end{bmatrix} \delta_2 \begin{bmatrix} \beta_1 & 0 & 0 \\ 0 & I & 0 \\ 0 & 0 & I \end{bmatrix} = \quad (21)$$

$$\begin{bmatrix} \beta_1^T \bar{A}^T & \beta_2 + \beta_2^T \bar{A} \beta_1 & \beta_2^T \bar{D} & \beta_1^T \\ \bar{D} \beta_2 & \gamma^2 I & 0 & \\ \begin{bmatrix} C_1(t) & D_{12}(t)\hat{C} \end{bmatrix} \beta_1 & 0 & -I \end{bmatrix} < 0$$

C. The New Proposed Controller Design Steps

- 1) State-space related to the islanded microgrid
- 2) Determining φ_1, φ_2 , and φ_3 (Degrees of freedom).
- 3) Solving the linear matrix inequality (13 & 29) and $\Gamma_1, \Gamma_2, \Gamma_3, \Gamma_4, \Gamma_5, \Gamma_6, \Gamma_7, \Gamma_8, \Gamma_9, \Gamma_{10} > 0$ using YALMIP.
- 4) Obtaining $L_{n \times p}, K_{n \times n}, E_{n \times n}, S_{n \times n}, R_{n \times n}$ through Steps (2) and (3).
- 5) Determining N and M as $N=I$ and $M=I-RS$.

6) Obtaining the controller parameters via equation (23).

Fig. 5 shows the controller design steps for controlling virtual inertia in the islanded microgrid.

Results and Discussion

The Islanded microgrid parameters are shown in Table 1. Dynamic controller values for the islanded microgrid, according to the new proposed control method, are shown in the appendix section. Simulation has been considered in six scenarios in order to compare

the performance of the proposed controller for virtual inertia control with consideration of virtual damping in the microgrid. In scenario (1), load disturbance has been imposed upon the microgrid. In scenario (2), load disturbance has been imposed, considering uncertainty in microgrid parameters (inertia). In scenarios (3), (4), (5), (6) and (7), various disturbances, including load and distributed generation resources (wind farm, solar farm) have been imposed upon the islanded microgrid.

$$\delta_3 = \begin{bmatrix} A(t)R + RA^T(t) + M\hat{C}(t)B^T(t) & A(t) + RA^T(t)S + M\hat{C}^T(t)B^T(t)S & D(t) & RC_1^T(t) + M\hat{C}^T(t)D_{12}^T(t) \\ & + RC_2^T(t)\hat{B}^T(t)N^T + M\hat{A}^T(t)N^T & & \\ A^T(t) + SA(t)R + SB(t)\hat{C}M^T & A^T(t)S + SA(t) + N\hat{B}C_2(t)\hat{B}^T N^T & SD(t) & C_1^T(t) \\ + N\hat{B}(t)C_2(t) + N\hat{A}M^T & & & \\ & & & \\ D^T(t) & D^T(t)S & -\gamma^2 I & 0 \\ C_1(t)R + D_{12}(t)\hat{C}M^T & C_1(t) & 0 & -I \end{bmatrix} < 0 \quad (22)$$

$$\hat{A} = N^{-1}(E - LC_2R - SAR - SBK)M^{-T}, \hat{B} = N^{-1}L, \hat{C} = KM^{-T} \quad (23)$$

$$\delta_3 = \begin{bmatrix} AR + RA^T + BK + K^T B^T & A + E^T & D & RC_1^T + K^T D_{12}^T \\ A^T + E & A^T S + SA + LC_2 + C_2^T L^T & SD & C_1^T \\ D^T & D^T S & -\gamma^2 I & 0 \\ C_1 R + D_{12} K & C_1 & 0 & -I \end{bmatrix} + o_1 + o_2 + o_3 + o_4 + o_5 + o_6 + o_7 + o_8 + o_9 + o_{10} + o_{11} + o_{12} + o_{13} < 0$$

$$o_1 = \begin{bmatrix} \Delta AR + R\Delta A^T & 0 & 0 & 0 \\ 0 & 0 & 0 & 0 \\ 0 & 0 & 0 & 0 \\ 0 & 0 & 0 & 0 \end{bmatrix}, o_2 = \begin{bmatrix} \Delta BK + K^T \Delta B^T & 0 & 0 & 0 \\ 0 & 0 & 0 & 0 \\ 0 & 0 & 0 & 0 \\ 0 & 0 & 0 & 0 \end{bmatrix}, o_3 = \begin{bmatrix} 0 & \Delta A & 0 & 0 \\ \Delta A^T & 0 & 0 & 0 \\ 0 & 0 & 0 & 0 \\ 0 & 0 & 0 & 0 \end{bmatrix}, o_4 = \begin{bmatrix} 0 & R\Delta A^T S & 0 & 0 \\ S\Delta A^T R & 0 & 0 & 0 \\ 0 & 0 & 0 & 0 \\ 0 & 0 & 0 & 0 \end{bmatrix}$$

$$o_5 = \begin{bmatrix} 0 & K^T \Delta B^T S & 0 & 0 \\ S\Delta BK & 0 & 0 & 0 \\ 0 & 0 & 0 & 0 \\ 0 & 0 & 0 & 0 \end{bmatrix}, o_6 = \begin{bmatrix} 0 & R\Delta C_2^T L^T & 0 & 0 \\ L\Delta C_2 R & 0 & 0 & 0 \\ 0 & 0 & 0 & 0 \\ 0 & 0 & 0 & 0 \end{bmatrix}, o_7 = \begin{bmatrix} 0 & 0 & \Delta D & 0 \\ 0 & 0 & 0 & 0 \\ \Delta D^T & 0 & 0 & 0 \\ 0 & 0 & 0 & 0 \end{bmatrix}, o_8 = \begin{bmatrix} 0 & 0 & 0 & R\Delta C_1^T \\ 0 & 0 & 0 & 0 \\ 0 & 0 & 0 & 0 \\ \Delta C_1 R & 0 & 0 & 0 \end{bmatrix}$$

$$o_9 = \begin{bmatrix} 0 & 0 & 0 & K^T \Delta D_{12}^T \\ 0 & 0 & 0 & 0 \\ 0 & 0 & 0 & 0 \\ \Delta D_{12} K & 0 & 0 & 0 \end{bmatrix}, o_{10} = \begin{bmatrix} 0 & 0 & 0 & 0 \\ 0 & \Delta A^T S + S\Delta A & 0 & 0 \\ 0 & 0 & 0 & 0 \\ 0 & 0 & 0 & 0 \end{bmatrix}, o_{11} = \begin{bmatrix} 0 & 0 & 0 & 0 \\ 0 & L\Delta C_2 + \Delta C_2^T L^T & 0 & 0 \\ 0 & 0 & 0 & 0 \\ 0 & 0 & 0 & 0 \end{bmatrix}, o_{12} = \begin{bmatrix} 0 & 0 & 0 & 0 \\ 0 & 0 & S\Delta D & 0 \\ 0 & \Delta D^T S & 0 & 0 \\ 0 & 0 & 0 & 0 \end{bmatrix}$$

$$o_{13} = \begin{bmatrix} 0 & 0 & 0 & 0 \\ 0 & 0 & 0 & \Delta C_1^T \\ 0 & 0 & 0 & 0 \\ 0 & 0 & \Delta C_1 & 0 \end{bmatrix}, o = \begin{bmatrix} AR + RA^T + BK + K^T B^T & A + E^T & D & RC_1^T + K^T D_{12}^T \\ A^T + E & A^T S + SA + LC_2 + C_2^T L^T & SD & C_1^T \\ D^T & D^T S & -\gamma^2 I & 0 \\ C_1 R + D_{12} K & C_1 & 0 & -I \end{bmatrix}$$

$$\sigma F v + v^T F^T \sigma^T \leq \Gamma \sigma \sigma^T + \Gamma^{-1} v^T v, F^T F \leq I \quad (25)$$

$$\begin{aligned}
 o_1 &= \sigma_1 F v_1 + v_1^T F^T \sigma_1^T \leq \Gamma_1 \sigma_1 \sigma_1^T + \Gamma_1^{-1} v_1^T v_1, & o_2 &= \sigma_2 F v_2 + v_2^T F^T \sigma_2^T \leq \Gamma_2 \sigma_2 \sigma_2^T + \Gamma_2^{-1} v_2^T v_2 \\
 o_3 &= \sigma_3 F v_3 + v_3^T F^T \sigma_3^T \leq \Gamma_3 \sigma_3 \sigma_3^T + \Gamma_3^{-1} v_3^T v_3, & o_4 &= \sigma_4 F v_4 + v_4^T F^T \sigma_4^T \leq \Phi_1 \sigma_4 \sigma_4^T + \Phi_1^{-1} v_4^T v_4 \\
 o_5 &= \sigma_5 F v_5 + v_5^T F^T \sigma_5^T \leq \Phi_2 \sigma_5 \sigma_5^T + \Phi_2^{-1} v_5^T v_5, & o_6 &= \sigma_6 F v_6 + v_6^T F^T \sigma_6^T \leq \Phi_3 \sigma_6 \sigma_6^T + \Phi_3^{-1} v_6^T v_6 \\
 o_7 &= \sigma_7 F v_7 + v_7^T F^T \sigma_7^T \leq \Gamma_4 \sigma_7 \sigma_7^T + \Gamma_4^{-1} v_7^T v_7, & o_8 &= \sigma_8 F v_8 + v_8^T F^T \sigma_8^T \leq \Gamma_5 \sigma_8 \sigma_8^T + \Gamma_5^{-1} v_8^T v_8 \\
 o_9 &= \sigma_9 F v_9 + v_9^T F^T \sigma_9^T \leq \Gamma_6 \sigma_9 \sigma_9^T + \Gamma_6^{-1} v_9^T v_9, & o_{10} &= \sigma_{10} F v_{10} + v_{10}^T F^T \sigma_{10}^T \leq \Gamma_7 \sigma_{10} \sigma_{10}^T + \Gamma_7^{-1} v_{10}^T v_{10} \\
 o_{11} &= \sigma_{11} F v_{11} + v_{11}^T F^T \sigma_{11}^T \leq \Gamma_8 \sigma_{11} \sigma_{11}^T + \Gamma_8^{-1} v_{11}^T v_{11}, & o_{12} &= \sigma_{12} F v_{12} + v_{12}^T F^T \sigma_{12}^T \leq \Gamma_9 \sigma_{12} \sigma_{12}^T + \Gamma_9^{-1} v_{12}^T v_{12} \\
 o_{13} &= \sigma_{13} F v_{13} + v_{13}^T F^T \sigma_{13}^T \leq \Gamma_{10} \sigma_{13} \sigma_{13}^T + \Gamma_{10}^{-1} v_{13}^T v_{13}
 \end{aligned}$$

$$\begin{aligned}
 \sigma_1 &= \begin{bmatrix} M_A \\ 0 \\ 0 \\ 0 \end{bmatrix}, v_1 = [N_A R \quad 0 \quad 0 \quad 0], \sigma_2 = \begin{bmatrix} M_B \\ 0 \\ 0 \\ 0 \end{bmatrix}, v_2 = [0 \quad N_A \quad 0 \quad 0] \\
 \sigma_3 &= \begin{bmatrix} M_A \\ 0 \\ 0 \\ 0 \end{bmatrix}, v_3 = [0 \quad N_A \quad 0 \quad 0], \sigma_4 = \begin{bmatrix} 0 \\ S M_A \\ 0 \\ 0 \end{bmatrix}, v_4 = [N_A R \quad 0 \quad 0 \quad 0] \\
 \sigma_5 &= \begin{bmatrix} 0 \\ S M_B \\ 0 \\ 0 \end{bmatrix}, v_5 = [N_B K \quad 0 \quad 0 \quad 0], \sigma_6 = \begin{bmatrix} 0 \\ L M_{C_2} \\ 0 \\ 0 \end{bmatrix}, v_6 = [N_{C_2} R \quad 0 \quad 0 \quad 0] \\
 \sigma_7 &= \begin{bmatrix} M_D \\ 0 \\ 0 \\ 0 \end{bmatrix}, v_7 = [0 \quad 0 \quad N_D \quad 0], \sigma_8 = \begin{bmatrix} 0 \\ 0 \\ 0 \\ M_{C_1} \end{bmatrix}, v_8 = [N_{C_1} R \quad 0 \quad 0 \quad 0] \\
 \sigma_9 &= \begin{bmatrix} 0 \\ 0 \\ 0 \\ M_{D_{12}} \end{bmatrix}, v_9 = [N_{D_{12}} K \quad 0 \quad 0 \quad 0], \sigma_{10} = \begin{bmatrix} 0 \\ S M_A \\ 0 \\ 0 \end{bmatrix}, v_{10} = [0 \quad N_A \quad 0 \quad 0] \\
 \sigma_{11} &= \begin{bmatrix} 0 \\ L M_{C_2} \\ 0 \\ 0 \end{bmatrix}, v_{11} = [0 \quad N_{C_2} \quad 0 \quad 0], \sigma_{12} = \begin{bmatrix} 0 \\ S M_D \\ 0 \\ 0 \end{bmatrix}, v_{12} = [0 \quad 0 \quad N_D \quad 0] \\
 \sigma_{13} &= \begin{bmatrix} 0 \\ 0 \\ 0 \\ M_{C_1} \end{bmatrix}, v_{13} = [0 \quad N_{C_1} \quad 0 \quad 0], \bar{o}_1 = \Gamma_1 \sigma_1 \sigma_1^T + \Gamma_1^{-1} v_1^T v_1, \bar{o}_2 = \Gamma_2 \sigma_2 \sigma_2^T + \Gamma_2^{-1} v_2^T v_2 \\
 \bar{o}_3 &= \Gamma_3 \sigma_3 \sigma_3^T + \Gamma_3^{-1} v_3^T v_3, \bar{o}_4 = \Phi_1 \sigma_4 \sigma_4^T + \Phi_1^{-1} v_4^T v_4, \bar{o}_5 = \Phi_2 \sigma_5 \sigma_5^T + \Phi_2^{-1} v_5^T v_5, \bar{o}_6 = \Phi_3 \sigma_6 \sigma_6^T + \Phi_3^{-1} v_6^T v_6 \\
 \bar{o}_7 &= \Gamma_4 \sigma_7 \sigma_7^T + \Gamma_4^{-1} v_7^T v_7, \bar{o}_8 = \Gamma_5 \sigma_8 \sigma_8^T + \Gamma_5^{-1} v_8^T v_8, \bar{o}_9 = \Gamma_6 \sigma_9 \sigma_9^T + \Gamma_6^{-1} v_9^T v_9, \bar{o}_{10} = \Gamma_7 \sigma_{10} \sigma_{10}^T + \Gamma_7^{-1} v_{10}^T v_{10} \\
 \bar{o}_{11} &= \Gamma_8 \sigma_{11} \sigma_{11}^T + \Gamma_8^{-1} v_{11}^T v_{11}, \bar{o}_{12} = \Gamma_9 \sigma_{12} \sigma_{12}^T + \Gamma_9^{-1} v_{12}^T v_{12}, \bar{o}_{13} = \Gamma_{10} \sigma_{13} \sigma_{13}^T + \Gamma_{10}^{-1} v_{13}^T v_{13}
 \end{aligned}$$

(26)

$$\delta_3 \leq o + \sum_{i=1}^{13} o_i^- = \delta_4 < 0 \quad (27)$$

$$\delta_4 = o + \sum_{i=2}^{13} o_i^- + \begin{bmatrix} \Gamma_1 M_A M_A^T & 0 & 0 & 0 \\ 0 & 0 & 0 & 0 \\ 0 & 0 & 0 & 0 \\ 0 & 0 & 0 & 0 \end{bmatrix} + \begin{bmatrix} RN_A^T \\ 0 \\ 0 \\ 0 \end{bmatrix} \Gamma_1^{-1} [N_A R \ 0 \ 0 \ 0] < 0 \quad (28)$$

$$\delta_4 = \begin{bmatrix} o + \sum_{i=2}^{13} o_i^- \\ [N_A R \ 0 \ 0 \ 0] \end{bmatrix} \begin{bmatrix} RN_A^T \\ 0 \\ 0 \\ 0 \\ -\Gamma_1 \end{bmatrix} < 0$$

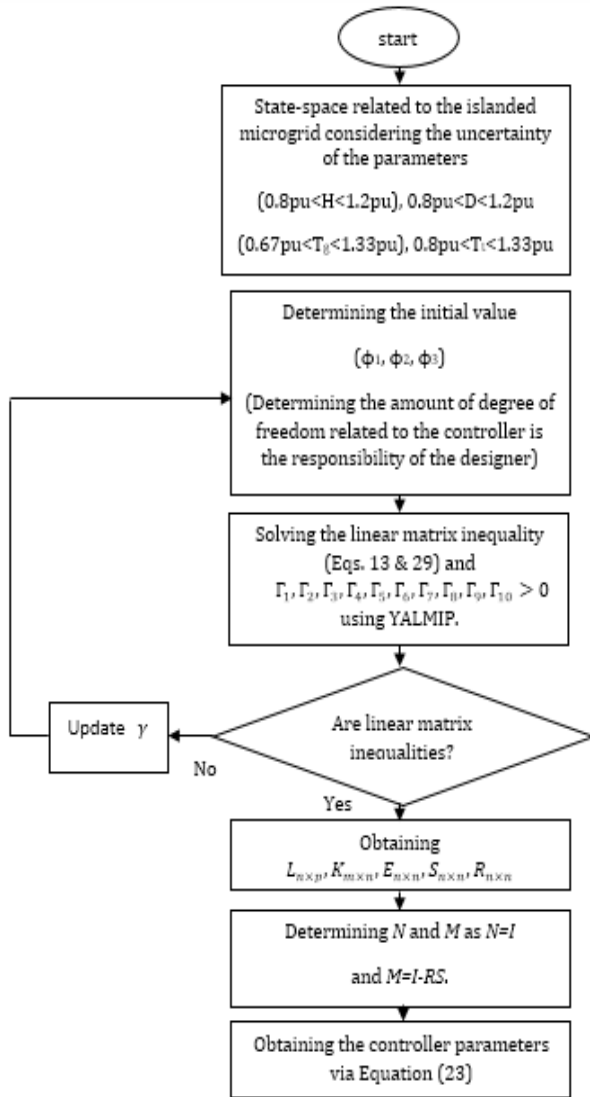


Fig. 5: : The controller design steps for controlling virtual inertia in the islanded microgrid.

Scenario (1): In this scenario, load disturbance of $\Delta P_{L1}=0.1pu$ at the time of $t=1$ has been imposed upon the islanded microgrid [25]. In Fig. 6, the microgrid

frequency deviation using various controllers has been depicted. The frequency deviation using the proposed control method is 0.02 Hz. The frequency deviation using the pi-optimizer controller (with virtual inertia and virtual damping) method is 0.12 Hz. frequency deviation using the no controller (with virtual inertia and virtual damping) method is 0.24 Hz, and frequency deviation using the no controller (with virtual inertia) method is 0.26 Hz [25]. According to Fig. 6, the new proposed robust controller shows desirable performance against disturbances, compared to other methods (no controller (with virtual inertia and virtual damping), no controller (with virtual inertia), and pi-optimizer controller (with virtual inertia and virtual damping)). Using the proposed controller, the settling time of frequency deviation is 5.25 seconds. Using the pi-optimizer controller, the settling time of the frequency deviation is 7.16 seconds. Using the no controller (with virtual inertia and virtual damping) method, the settling time of frequency deviation is 8.13 seconds. Using the no controller (virtual inertia) method, the settling time of frequency deviation is 13.44 seconds. The proposed method performs better than other mentioned controllers in terms of damping speed related to microgrid frequency fluctuations.

Scenario (2): In this scenario, load disturbance of $\Delta P_{L1}=0.1pu$ at the time of $t=1$, with the uncertainty of islanded microgrid parameters (-20% inertia), has been imposed upon the islanded microgrid. In Fig. 7, the microgrid frequency deviation using various controllers has been depicted. The frequency deviation using the proposed control method is 0.02 Hz. The frequency deviation using the pi-optimizer controller (with virtual inertia and virtual damping) method is 0.135 Hz. The frequency deviation using the no controller (with virtual inertia and virtual damping) method is 0.27 Hz, and frequency deviation using the no controller (with virtual inertia) method is 0.28 Hz [25]. According to Fig. 7, the new proposed robust controller shows desirable performance against disturbances and uncertainty of islanded microgrid parameters, compared to other

methods. Using the proposed controller, the settling time of the frequency deviation is 5.33 seconds. Using the pi-optimizer controller, the settling time of frequency deviations is 7.42 seconds. Using the no controller (with virtual inertia and virtual damping) method, the settling time of frequency deviation is 9.34 seconds. Using the no controller (virtual inertia) method, the settling time of frequency deviation is 14.51 seconds. The proposed method performs better than other mentioned controllers in terms of damping speed of

frequency fluctuations against the uncertainty of microgrid parameters.

Scenario (3): In this scenario, according to Fig. 8, load and distributed generation resource disturbances, with regard to the uncertainty of islanded microgrid parameters (-20% inertia, -20% damping), have been imposed upon the islanded microgrid [25]. In Fig. 9, the microgrid frequency deviation using various controllers has been depicted. According to Fig. 9, the new proposed robust controller shows desirable performance against disturbances and uncertainty of islanded microgrid parameters, compared to other methods (of no controller (with virtual inertia and virtual damping), no controller (with virtual inertia), and pi-optimizer controller (with virtual inertia and virtual damping)). The maximum frequency deviation using the proposed control method is 0.03 Hz. The maximum frequency deviation using the pi-optimizer controller (with virtual inertia and virtual damping) method is 0.10 Hz. The maximum frequency deviation using the no controller (with virtual inertia and virtual damping) method is 0.22 Hz, and the maximum frequency deviation using the no controller (with virtual inertia) method is 0.26 Hz [25]. According to the results of this scenario, the proposed controller has been able to reduce the frequency error due to load and distributed generation resource disturbances and compared to other controllers; this frequency deviation has been reduced by 68%.

Scenario (4): In this scenario, according to Fig. 8, load and distributed generation resource disturbances, with regard to the uncertainty of islanded microgrid parameters (-20% inertia, -20% damping, +33% Time constant of governor), have been imposed upon the islanded microgrid. In Fig. 10, the microgrid frequency deviation using various controllers is shown. Frequency deviation using the proposed control method is 0.03 Hz. The frequency deviation using the pi-optimizer controller (with virtual inertia and virtual damping) method is 0.11 Hz.

The frequency deviation using the no controller (with virtual inertia and virtual damping) method is 0.31 Hz, and the frequency deviation using the no controller (with virtual inertia) method is 0.39 Hz. Looking at the results, it can be said that the proposed controller has had a

good performance in weakening the disturbance caused by the load and distributed generation resources disturbances and has been able to reduce the frequency error by 72%.

Scenario (5): In this scenario, according to Fig. 8, load and distributed generation resource disturbances, with regard to the uncertainty of islanded microgrid parameters (-20% inertia, -20% damping, +33% Time constant of governor, -33% Time constant of Turbine), have been imposed upon the islanded microgrid. In Fig. 11, the microgrid frequency deviation using various controllers is shown. The maximum Frequency deviation using the proposed control method is 0.033 Hz. The maximum frequency deviation using the pi-optimizer controller (with virtual inertia and virtual damping) method is 0.14 Hz. The maximum frequency deviation using the no controller (with virtual inertia and virtual damping) method is 0.35 Hz, and the maximum frequency deviation using the no controller (with virtual inertia) method is 0.45 Hz. The results of this scenario show that the proposed controller is also robust to severe uncertainties, and the frequency error is reduced by 72% compared to the other mentioned control methods.

Scenario (6): In this scenario, according to Fig. 12, load and distributed generation resource disturbances, have been imposed upon the islanded microgrid [21]. In Fig. 13, the microgrid frequency deviation using various controllers is shown. The maximum Frequency deviation using the proposed control method is 0.045 Hz. The maximum frequency deviation using the Self-adaptive virtual inertia control using fuzzy logic is 0.19 Hz [21], and the maximum frequency deviation using the MPC controller (with virtual inertia and virtual damping) is 0.28 Hz [23].

According to the results of this scenario, the MPC controller and Self-adaptive virtual inertia control do not perform well against disturbance, and the effect of disturbance on the microgrid frequency is high. While the proposed controller has been able to greatly weaken the disturbance effect, the frequency error has been reduced by 75% compared to other controllers.

Scenario (7): In this scenario, according to Fig. 12 load and distributed generation resource disturbances, with regard to the uncertainty of islanded microgrid parameters (-20% inertia), have been imposed upon the islanded microgrid. In Fig. 14, the microgrid frequency deviation using various controllers is shown. The maximum Frequency deviation using the proposed control method is 0.054 Hz.

The maximum frequency deviation using the Self-adaptive virtual inertia control using fuzzy logic is 0.21 Hz [21], and maximum frequency deviation using the MPC controller [23] (with virtual inertia and virtual

damping) is 0.30 Hz. According to the results of this scenario, the proposed controller has a better performance than the new controllers used in the field of virtual inertia control.

Conclusion

In microgrids, power electronic converters are utilized for power exchange and possess very low inertia compared to power systems. Therefore, a virtual synchronous generator is used for implementing large synchronous generator behavior in a power system, which provides desirable inertia for the system.

Virtual inertia control is a component of the virtual synchronous generator which helps improve microgrid frequency stability. In microgrids with vast energy resources, in addition to virtual inertia, considering virtual damping can reduce system instability. In this paper, designing a new robust control method for controlling virtual inertia in microgrids, with regard to virtual damping, has been attempted. The proposed control method does not require measuring of all the modes and uses only output feedback. According to the simulation results, the proposed controller has a better performance than other controllers in improving the frequency stability of the islanded microgrid.

$$\begin{bmatrix}
 \delta_{1_{mn}} & A+E^T & D & RC_1^T + KD_{12}^T & RN_A^T & K^T N_B^T & 0_{n \times 1} & 0_{n \times 1} & RN_{C_1}^T & KN_{D_{12}}^T & 0_{n \times 1} & RN_A^T & 0_{n \times 1} & K^T N_B^T & 0_{n \times 1} & RN_{C_2}^T \\
 A^T + E & \delta_{22_{mn}} & SD & C_1^T & 0_{n \times 1} & 0_{n \times 1} & N_A^T & 0_{n \times 1} & 0_{n \times 1} & 0_{n \times 1} & SM_A & LM_{C_2} & SN_D & N_{C_1}^T & SM_A & 0_{n \times 1} & SM_B & 0_{n \times 1} & LM_{C_2} & 0_{n \times 1} \\
 D & D^T S & \delta_{33_{d,d}} & 0_{d \times q} & 0_{d \times 1} & 0_{d \times 1} & N_D^T & 0_{d \times 1} \\
 C_1 R + D_{12} K & C_1 & 0_{q \times d} & \delta_{44_{q,q}} & 0_{q \times 1} \\
 N_A R & 0_{1 \times n} & 0_{1 \times d} & 0_{1 \times q} & -\Gamma_1 & 0 & 0 & 0 & 0 & 0 & 0 & 0 & 0 & 0 & 0 & 0 & 0 & 0 & 0 & 0 \\
 N_B K & 0_{1 \times n} & 0_{1 \times d} & 0_{1 \times q} & 0 & -\Gamma_2 & 0 & 0 & 0 & 0 & 0 & 0 & 0 & 0 & 0 & 0 & 0 & 0 & 0 & 0 \\
 0_{1 \times n} & N_A & 0_{1 \times d} & 0_{1 \times q} & 0 & 0 & -\Gamma_3 & 0 & 0 & 0 & 0 & 0 & 0 & 0 & 0 & 0 & 0 & 0 & 0 & 0 \\
 0_{1 \times n} & 0_{1 \times n} & N_D & 0_{1 \times q} & 0 & 0 & 0 & -\Gamma_4 & 0 & 0 & 0 & 0 & 0 & 0 & 0 & 0 & 0 & 0 & 0 & 0 \\
 N_{C_1} R & 0_{1 \times n} & 0_{1 \times d} & 0_{1 \times q} & 0 & 0 & 0 & 0 & -\Gamma_5 & 0 & 0 & 0 & 0 & 0 & 0 & 0 & 0 & 0 & 0 & 0 \\
 N_{D_{12}} K & 0_{1 \times n} & 0_{1 \times d} & 0_{1 \times q} & 0 & 0 & 0 & 0 & 0 & -\Gamma_6 & 0 & 0 & 0 & 0 & 0 & 0 & 0 & 0 & 0 & 0 \\
 0_{1 \times n} & M_A^T S & 0_{1 \times d} & 0_{1 \times q} & 0 & 0 & 0 & 0 & 0 & 0 & -\Gamma_7 & 0 & 0 & 0 & 0 & 0 & 0 & 0 & 0 & 0 \\
 0_{1 \times n} & M_{C_2}^T L^T & 0_{1 \times d} & 0_{1 \times q} & 0 & 0 & 0 & 0 & 0 & 0 & 0 & -\Gamma_8 & 0 & 0 & 0 & 0 & 0 & 0 & 0 & 0 \\
 0_{1 \times n} & M_D^T S & 0_{1 \times d} & 0_{1 \times q} & 0 & 0 & 0 & 0 & 0 & 0 & 0 & 0 & -\Gamma_9 & 0 & 0 & 0 & 0 & 0 & 0 & 0 \\
 0_{1 \times n} & N_{C_1} & 0_{1 \times d} & 0_{1 \times q} & 0 & 0 & 0 & 0 & 0 & 0 & 0 & 0 & 0 & -\Gamma_{10} & 0 & 0 & 0 & 0 & 0 & 0 \\
 0_{1 \times n} & M_A^T S & 0_{1 \times d} & 0_{1 \times q} & 0 & 0 & 0 & 0 & 0 & 0 & 0 & 0 & 0 & 0 & -\Phi_1^{-1} & 0 & 0 & 0 & 0 & 0 \\
 N_A R & 0_{1 \times n} & 0_{1 \times d} & 0_{1 \times q} & 0 & 0 & 0 & 0 & 0 & 0 & 0 & 0 & 0 & 0 & 0 & -\Phi_1 & 0 & 0 & 0 & 0 \\
 0_{1 \times n} & M_B^T S & 0_{1 \times d} & 0_{1 \times q} & 0 & 0 & 0 & 0 & 0 & 0 & 0 & 0 & 0 & 0 & 0 & 0 & -\Phi_2^{-1} & 0 & 0 & 0 \\
 N_B K & 0_{1 \times n} & 0_{1 \times d} & 0_{1 \times q} & 0 & 0 & 0 & 0 & 0 & 0 & 0 & 0 & 0 & 0 & 0 & 0 & 0 & -\Phi_2 & 0 & 0 \\
 0_{1 \times n} & M_{C_2}^T L^T & 0_{1 \times d} & 0_{1 \times q} & 0 & 0 & 0 & 0 & 0 & 0 & 0 & 0 & 0 & 0 & 0 & 0 & 0 & 0 & -\Phi_3^{-1} & 0 \\
 N_{C_2} R & 0_{1 \times n} & 0_{1 \times d} & 0_{1 \times q} & 0 & 0 & 0 & 0 & 0 & 0 & 0 & 0 & 0 & 0 & 0 & 0 & 0 & 0 & 0 & -\Phi_3
 \end{bmatrix} < 0 \tag{29}$$

$$\begin{cases}
 \delta_{1_{mn}} = AR + RA^T + BK + K^T B^T + (\Gamma_1 + \Gamma_3)M_A M_A^T + \Gamma_2 M_B M_B^T + \Gamma_4 M_D M_D^T \\
 \delta_{22_{mn}} = A^T S + SA + LC_2 + C_2^T L^T + \Gamma_7 N_A^T N_A + \Gamma_8 N_{C_2}^T N_{C_2}, \delta_{33_{d,d}} = -\gamma^2 I + \Gamma_9 N_D^T N_D \\
 \delta_{44_{q,q}} = -I + (\Gamma_5 + \Gamma_{10})M_{C_1} M_{C_1}^T + \Gamma_6 M_{D_{12}} M_{D_{12}}^T
 \end{cases}$$

Table 1: The Islanded microgrid parameters [24], [25]

Parameter	value	Parameter	value
Virtual damping, $D_{VI}(s)$	1.2	Governor Time constant, $T_g(s)$	0.1
Time constant of ESS, $T_{ESS}(s)$	10	Turbine Time constant, $T_t(s)$	0.4
Time constant of wind turbine, $T_{WT}(s)$	1.4	Drop factor, R (Hz/pu. MW)	2.4
Time constant of solar system, $T_{PV}(s)$	1.9	Virtual inertia, $J_{VI}(s)$	1.6
System (microgrid) inertia, H (p.u.MW s)	0.082	Secondary frequency controller, $K(s)$	0.2
System (microgrid) damping, D (p.u.MW/Hz)	0.016	Frequency bias,	0.99

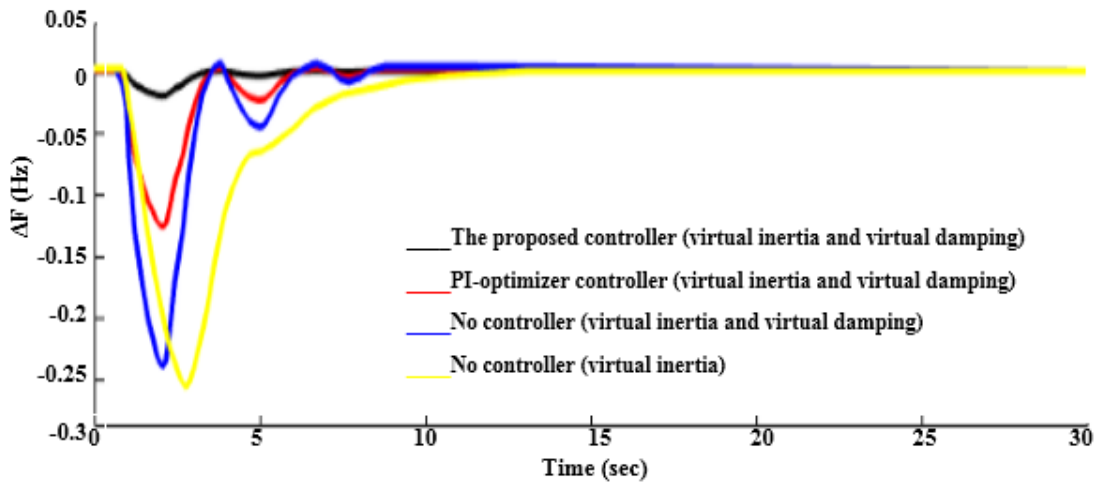


Fig. 6: The frequency deviation using various controllers, Scenario (1).

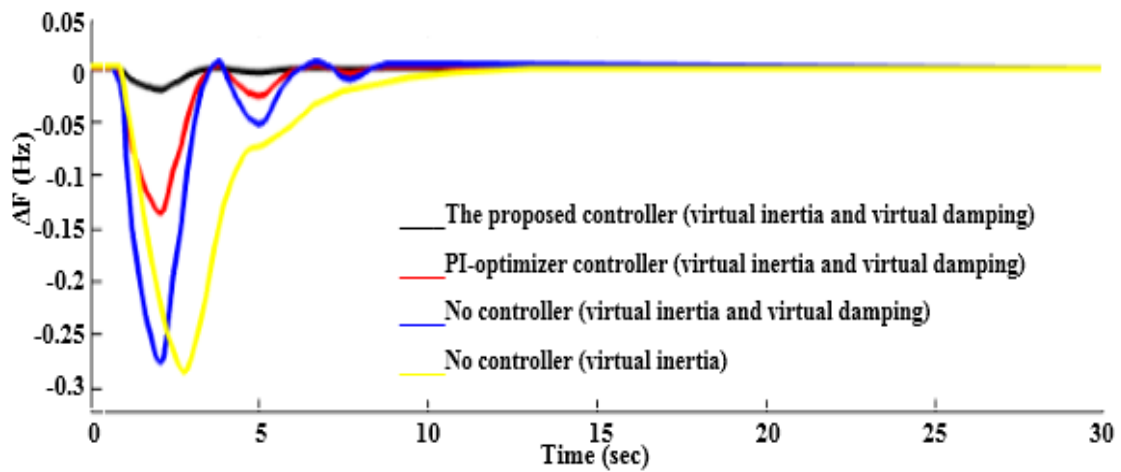


Fig. 7: The frequency deviation using various controllers, Scenario (2).

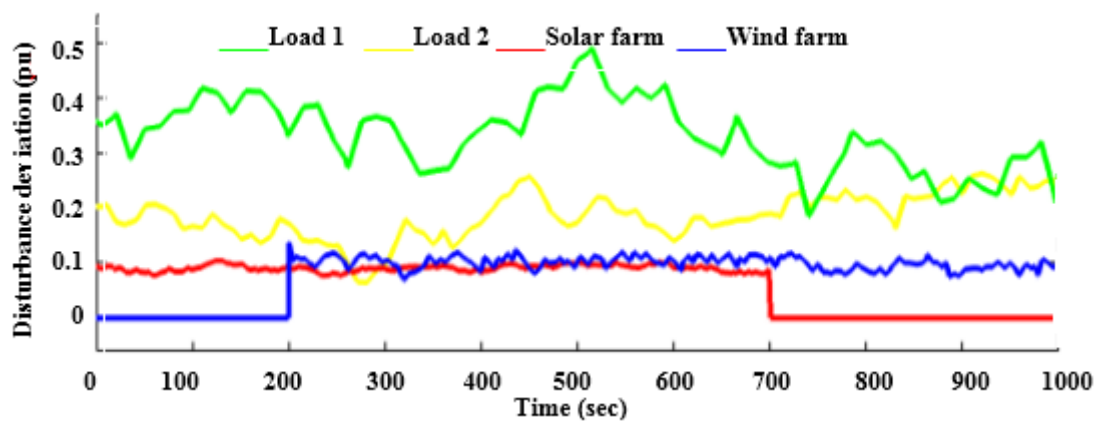


Fig. 8: Disturbances on the islanded microgrid [22]-[25].

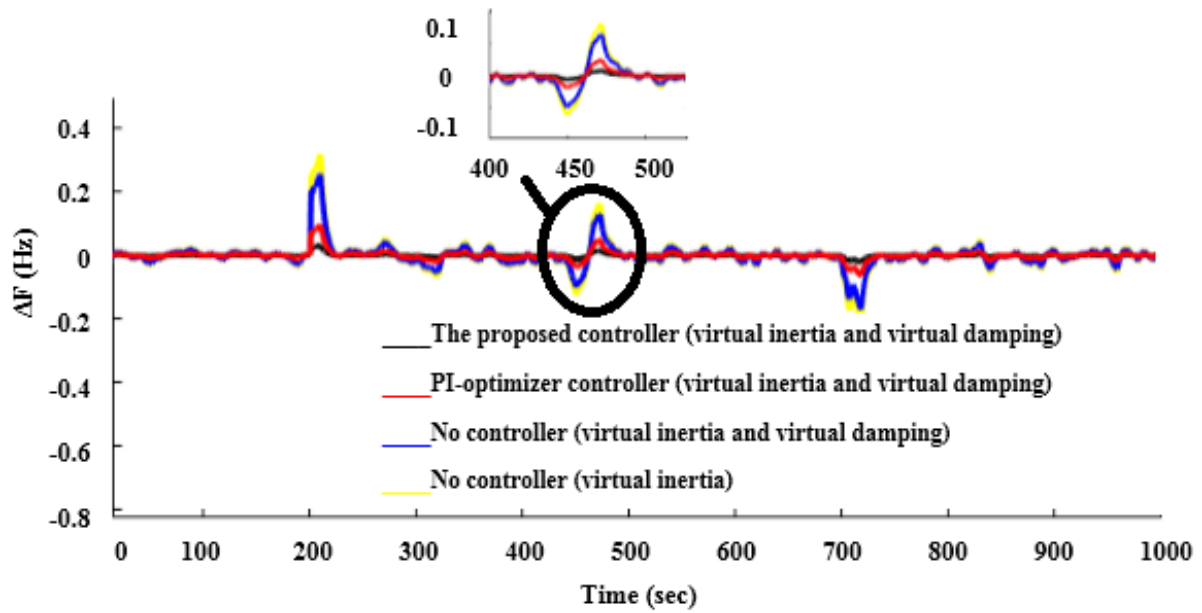


Fig. 9: : The frequency deviation using various controllers, Scenario (3).

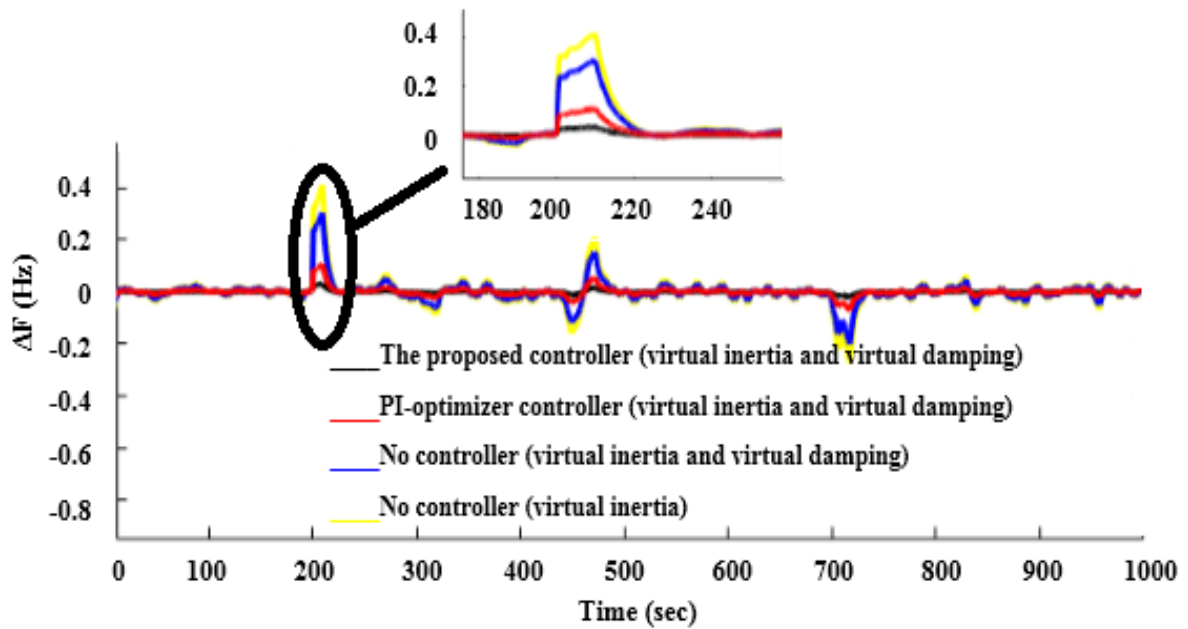


Fig. 10: : The frequency deviation using various controllers, Scenario (4).

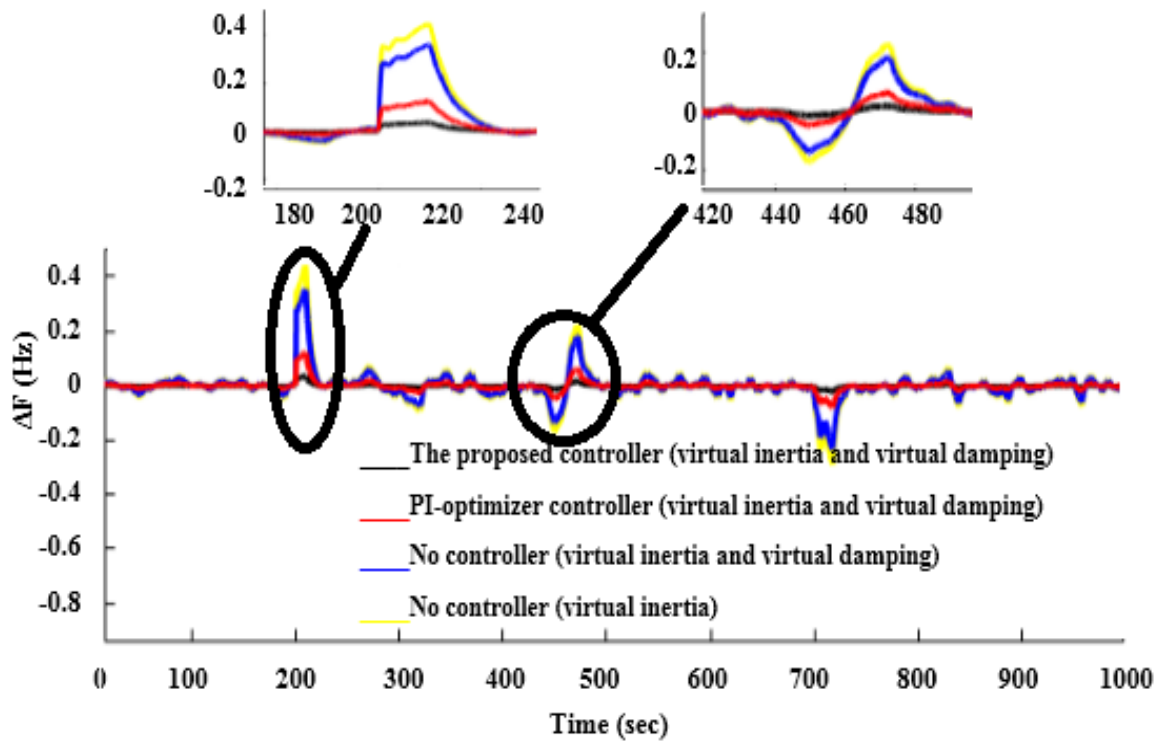


Fig. 11: The frequency deviation using various controllers, Scenario (5).

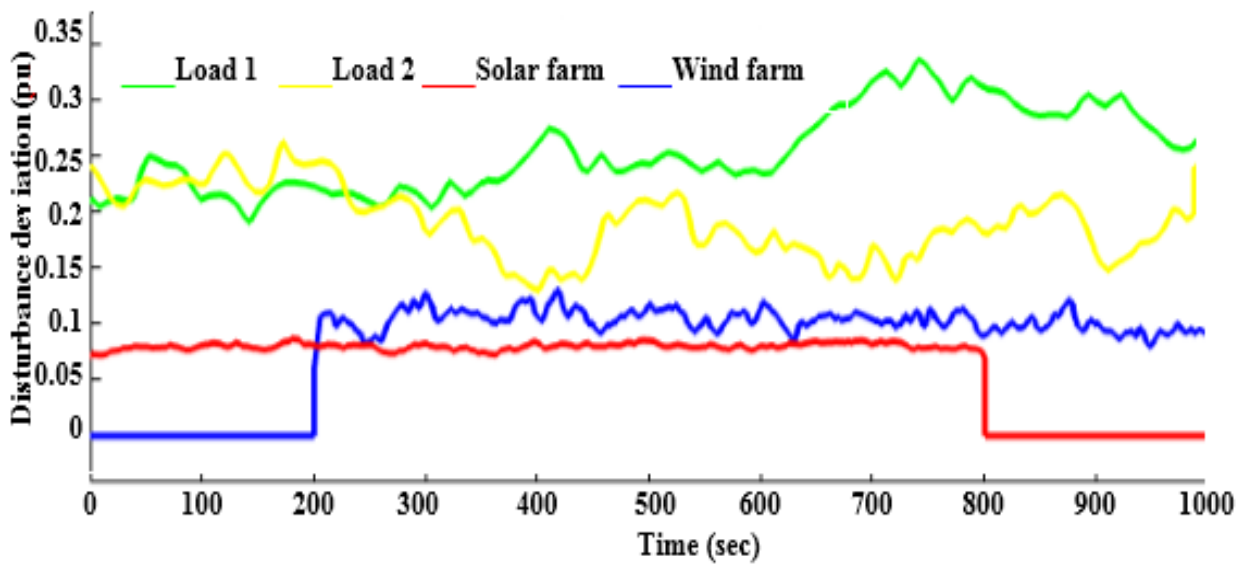


Fig. 12: Disturbances on the islanded microgrid, Scenario (6) [21].

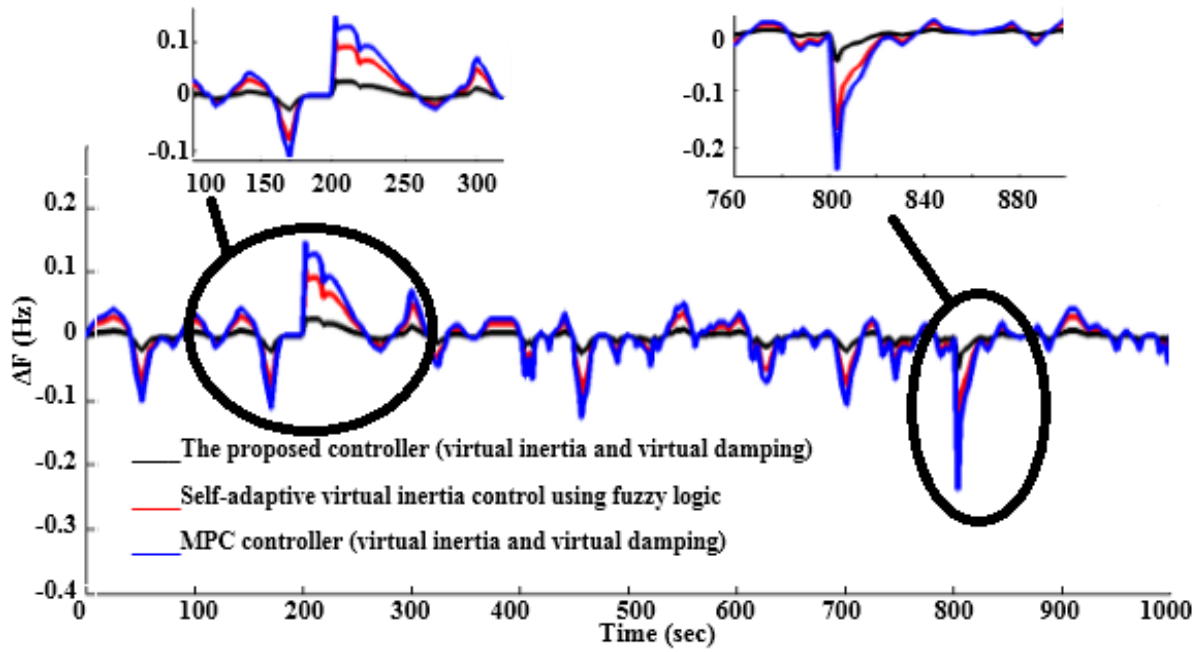


Fig. 13: The frequency deviation using various controllers, Scenario (6).

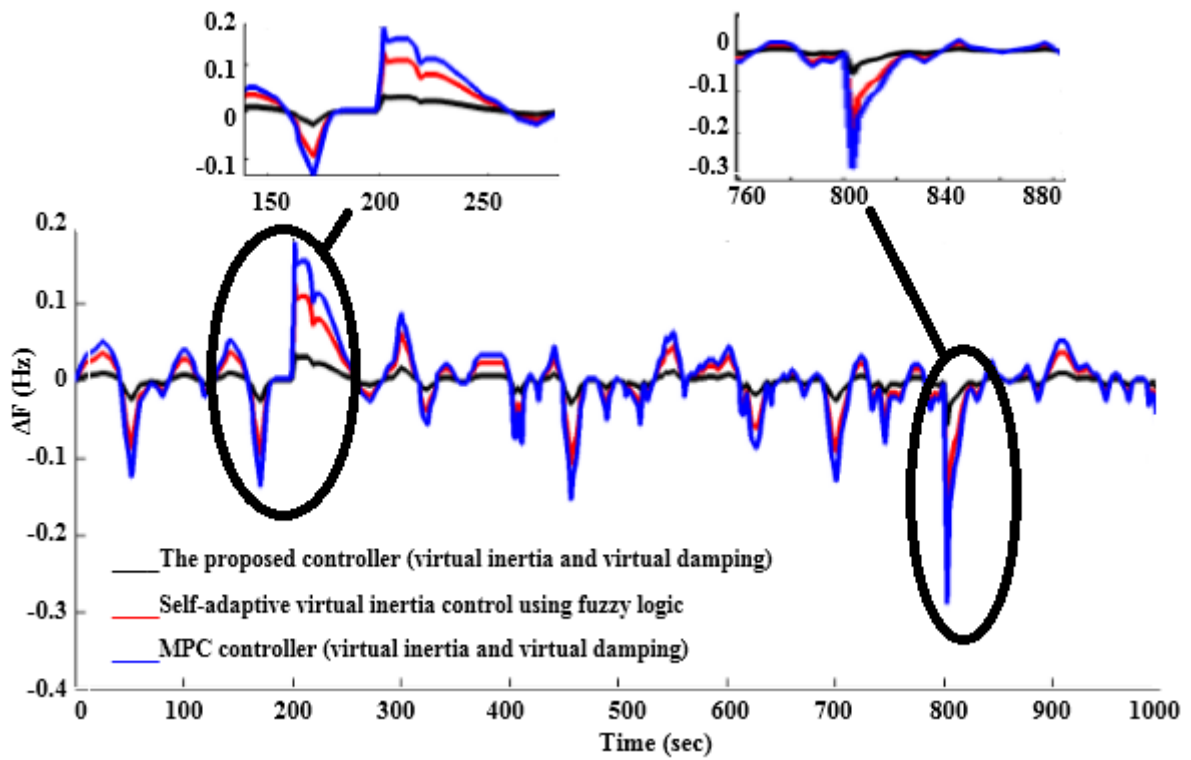


Fig. 14: : The frequency deviation using various controllers, Scenario (7).

Appendix

The proposed controller parameters shown in the appendix can greatly weaken the load disturbances and distributed generation resources disturbances in the islanded microgrid. These dynamic control parameters

$$\hat{A} = \begin{bmatrix} -176.07 & 4.4335 & 1.3472 & 0.7497 & 0.48059 & 178.08 & 129.61 \\ -130.79 & -5.9675 & 9.9792 & -0.75207 & -0.47191 & -178.53 & -129.96 \\ 21.59 & -0.052115 & -10.55 & 0.087908 & 0.054885 & 20.866 & 15.187 \\ 4809.6 & 176.53 & 73.776 & 30.808 & 19.36 & 7313.8 & 5324.1 \\ -18854 & -68397 & -29366 & -12092 & -7598.9 & -28706 & -20897 \\ -200.52 & -7.2778 & -3.1252 & -1.2864 & -0.80849 & -306.16 & -222.35 \\ -206.71 & -7.5025 & -3.2217 & -1.3262 & -0.83348 & -314.89 & -229.75 \end{bmatrix}, \hat{B} = \begin{bmatrix} -25167 \\ -49106 \\ 90292 \\ 25188 \\ -4813.4 \\ -54.716 \\ -55.91 \end{bmatrix}$$

$$\hat{C} = [21.077 \quad 0.76462 \quad 0.32829 \quad 0.13518 \quad 0.084949 \quad 32.091 \quad 23.361]$$

Author Contributions

F. Amiri and M. H. Moradi designed the island microgrid model and controller. F. Amiri collected the data and carried out the data analysis. F. Amiri interpreted the results and wrote the manuscript.

Conflict of Interest

The author declares that there is no conflict of interests regarding the publication of this manuscript. In addition, the ethical issues, including plagiarism, informed consent, misconduct, data fabrication and/or falsification, double publication and/or submission, and redundancy have been completely observed by the authors.

References

- [1] G. Yang, Y. Jia, M. Qin, Y. Fang, "Research of low voltage shore power supply used on shipping based on sliding control," *Journal of Electrical and Computer Engineering Innovations*, 4(1): 85-93, 2016.
- [2] A. Movahednasab, M. Rashidinejad, A. Abdollahi, "Market Based Analysis of Natural Gas and Electricity Export via System Dynamics," *Journal of Electrical and Computer Engineering Innovations*, 5(2): 109-120, 2017.
- [3] H. Amiri, G. A. Markadeh, N. Mahdian, "Voltage control and load sharing in a DC Islanded Microgrid Based on Disturbance Observer," *Journal of Electrical and Computer Engineering Innovations*, 7(1): 1-10, 2019.
- [4] M. Feli, F. Parandin, "A Numerical Optimization of an Efficient Double Junction InGaN/CIGS Solar Cell," *Journal of Electrical and Computer Engineering Innovations*, 6(1): 53-58, 2018.
- [5] M. HojatyDana, M. AlizadehPahlavani, "Control-Strategies-for-Performance-Assessment-of-an-Autonomous Wind Energy Conversion System. *Journal of Electrical and Computer Engineering Innovations*," 2(1): 15-20, 2014.
- [6] Li, X. Wang, J. Xiao, "Adaptive Event-Triggered Load Frequency Control for Interconnected Microgrids by Observer-Based Sliding Mode Control," in *IEEE Access*, 7: 68271-68280, 2019.
- [7] M. W. Siti, D. H. Tungadio, Y. Sun, N. T. Mbungu, R. Tiako, "Optimal frequency deviations control in microgrid interconnected systems," in *IET Renewable Power Generation*, 13(13): 2376-2382, 2019.
- [8] F. Amiri, M. H. Moradi, "Designing a Fractional Order PID Controller for a Two-Area Micro-Grid under Uncertainty of Parameters," *Iranian journal of energy* 20(4): 49-78, 2018.
- [9] F. Amiri, A. Hatami, "A Model Predictive Control Method for Load-Frequency Control in Islanded Microgrids," *Computational Intelligence in Electrical Engineering*, 8(1): 9-24, 2017.
- [10] F. Amiri, A. Hatami, "Nonlinear Load Frequency Control of Isolated Microgrid using Fractional Order PID Based on Hybrid Craziness-based Particle Swarm Optimization and Pattern Search," *Journal of Iranian Association of Electrical and Electronics Engineers*, 17(2): 135-148, 2020.
- [11] W. Wu et al., "A Virtual Inertia Control Strategy for DC Microgrids Analogized With Virtual Synchronous Machines," in *IEEE Transactions on Industrial Electronics*, 64(7): 6005-6016, 2017.
- [12] Ali et al. , "A New Frequency Control Strategy in an Islanded Microgrid Using Virtual Inertia Control-Based Coefficient Diagram Method," in *IEEE Access*, 7: 16979-16990, 2019.
- [13] Z. Yi, X. Zhao, D. Shi, J. Duan, Y. Xiang, Z. Wang, "Accurate Power Sharing and Synthetic Inertia Control for DC Building Microgrids With Guaranteed Performance," in *IEEE Access*, 7: 63698-63708, 2019.
- [14] J. Li, B. Wen, H. Wang, "Adaptive Virtual Inertia Control Strategy of VSG for Micro-Grid Based on Improved Bang-Bang Control Strategy," in *IEEE Access*, 7: 39509-39514, 2019.
- [15] J. Liu, M. J. Hossain, J. Lu, F. H. M. Rafi, H. Li, "A hybrid AC/DC microgrid control system based on a virtual synchronous generator for smooth transient performances," *Electric Power Systems Research*, 162: 169-182. 2018.
- [16] P. Li, W. Hu, X. Xu, Q. Huang, Z. Liu, Z. Chen, "A frequency control strategy of electric vehicles in microgrid using virtual synchronous generator control," *Energy*, 189: 116389, 2019.
- [17] Ali et al., "A New Frequency Control Strategy in an Islanded Microgrid Using Virtual Inertia Control-Based Coefficient Diagram Method," in *IEEE Access*, 7: 16979-16990, 2019.
- [18] X. Hou, Y. Sun, X. Zhang, J. Lu, P. Wang, J. M. Guerrero, "Improvement of Frequency Regulation in VSG-Based AC Microgrid Via Adaptive Virtual Inertia," in *IEEE Transactions on Power Electronics*, 35(2): 1589-1602, 2020.
- [19] K. Tan, F. Lin, C. Shih, C. Kuo, "Intelligent Control of Microgrid With Virtual Inertia Using Recurrent Probabilistic Wavelet Fuzzy Neural Network," in *IEEE Transactions on Power Electronics*, 35(7): 7451-7464, 2020.
- [20] T. Kerdpol, F. S. Rahman, Y. Mitani, M. Watanabe, S. K. Küfeoğlu, "Robust Virtual Inertia Control of an Islanded Microgrid Considering High Penetration of Renewable Energy," in *IEEE Access*, 6: 625-636, 2018.

- [21] T. Kerdphol, M. Watanabe, K. Hongesombut, Y. Mitani, "Self-Adaptive Virtual Inertia Control-Based Fuzzy Logic to Improve Frequency Stability of Microgrid With High Renewable Penetration," in IEEE Access, 7: 76071-76083, 2019.
- [22] T. Kerdphol, F. S. Rahman, M. Watanabe, Y. Mitani, "Robust Virtual Inertia Control of a Low Inertia Microgrid Considering Frequency Measurement Effects," in IEEE Access, 7: 57550-57560, 2019.
- [23] T. Kerdphol, F. S. Rahman, Y. Mitani, K. Hongesombut, S. Küfeoğlu, "Virtual inertia control-based model predictive control for microgrid frequency stabilization considering high renewable energy integration," Sustainability, 9(5): 773, 2017.
- [24] T. Kerdphol, F. S. Rahman, Y. Mitani, "Virtual inertia control application to enhance frequency stability of interconnected power systems with high renewable energy penetration," Energies, 11(4): 981, 2018.
- [25] T. Kerdphol, F. S. Rahman, M. Watanabe, Y. Mitani, D. Turschner, H. Beck, "Enhanced Virtual Inertia Control Based on Derivative Technique to Emulate Simultaneous Inertia and Damping Properties for Microgrid Frequency Regulation, " in IEEE Access, 7: 14422-14433, 2019.
- [26] C. Scherer, P. Gahinet, M. Chilali, "Multiobjective output-feedback control via LMI optimization," in IEEE Transactions on Automatic Control, 42(7): 896-911, 1997.
- [27] H. Li, X. Jing, H. R. Karimi, "Output-Feedback-Based H_∞ Control for Vehicle Suspension Systems With Control Delay, " in IEEE Transactions on Industrial Electronics, 61(1): 436-446, 2014.
- [28] D. Choi, C. K. Ahn, M. T. Lim, & M. K. Song, "Dynamic output-feedback H_∞ control for active half-vehicle suspension systems with time-varying input delay. International Journal of Control, Automation and Systems, 14(1): 59-68, 2016.

Biographies



Farhad Amiri was born in Ilam, Iran. He received the M.Sc. degree in Electrical Engineering from the university of Bu-Ali Sina at 2017. He is currently working toward the Ph.D. degree in Electrical Engineering at Bu-Ali Sina university. His research interests include Dynamic and Transient operation of power system, Control, Microgrid and Renewable Energy.



Mohammad Hassan Moradi was born in Nowshahr, Mazandaran, Iran. He obtained his B.Sc., M.Sc. and PhD from Sharif University of Technology, Tarbiat Modares University and Strathclyde University in Glasgow, Scotland in 1991 1993 and 2002 respectively. His research interests include New and Green Energy, Micro Grid Modeling and Control, DG Location and Sizing in Power System, photovoltaic systems and power electronics, Combined Heat and Power Plant, Power Quality, Supervisory Control, Fuzzy Control.

Copyrights

©2020 The author(s). This is an open access article distributed under the terms of the Creative Commons Attribution (CC BY 4.0), which permits unrestricted use, distribution, and reproduction in any medium, as long as the original authors and source are cited. No permission is required from the authors or the publishers.



How to cite this paper:

F. Amiri, M.H. Moradi, "Designing a new robust control for virtual inertia control in the microgrid with regard to virtual damping," Journal of Electrical and Computer Engineering Innovations, 8(1): 53-70, 2020.

DOI: [10.22061/JECEI.2020.6913.347](https://doi.org/10.22061/JECEI.2020.6913.347)

URL: http://jecei.sru.ac.ir/article_1423.html

